



**HAL**  
open science

## Enhanced Dielectric Relaxation in Self-Organized Layers of Polypeptides Coupled to Platinum Nanoparticles: Temperature Dependence and Effect of Bias Voltage

Louis Merle, Ghada Manai, Adeline Pham, Sébastien Lecommandoux, Philippe Demont, Colin Bonduelle, Simon Tricard, Adnen Mlayah, Jérémie Grisolia

### ► To cite this version:

Louis Merle, Ghada Manai, Adeline Pham, Sébastien Lecommandoux, Philippe Demont, et al.. Enhanced Dielectric Relaxation in Self-Organized Layers of Polypeptides Coupled to Platinum Nanoparticles: Temperature Dependence and Effect of Bias Voltage. *Journal of Physical Chemistry C*, 2021, 125 (41), pp.22643-22649. 10.1021/acs.jpcc.1c06457 . hal-03412910

**HAL Id: hal-03412910**

**<https://hal.science/hal-03412910v1>**

Submitted on 3 Nov 2021

**HAL** is a multi-disciplinary open access archive for the deposit and dissemination of scientific research documents, whether they are published or not. The documents may come from teaching and research institutions in France or abroad, or from public or private research centers.

L'archive ouverte pluridisciplinaire **HAL**, est destinée au dépôt et à la diffusion de documents scientifiques de niveau recherche, publiés ou non, émanant des établissements d'enseignement et de recherche français ou étrangers, des laboratoires publics ou privés.




## Open Archive Toulouse Archive Ouverte (OATAO)

OATAO is an open access repository that collects the work of Toulouse researchers and makes it freely available over the web where possible

This is an author's version published in: <http://oatao.univ-toulouse.fr/28419>

**Official URL:** <https://doi.org/10.1021/acs.jpcc.1c06457>

### **To cite this version:**

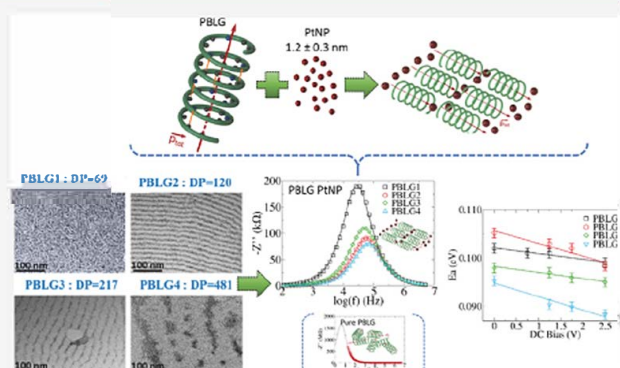
Merle, Louis and Manai, Ghada and Pham, Adeline and Lecommandoux, Sébastien and Demont, Philippe  and Bonduelle, Colin and Tricard, Simon and Mlayah, Adnen and Grisolia, Jérémie *Enhanced Dielectric Relaxation in Self-Organized Layers of Polypeptides Coupled to Platinum Nanoparticles: Temperature Dependence and Effect of Bias Voltage*. (2021) *Journal of Physical Chemistry C*, 125 (41). 1-7. ISSN 1932-7447

Any correspondence concerning this service should be sent to the repository administrator: [tech-oatao@listes-diff.inp-toulouse.fr](mailto:tech-oatao@listes-diff.inp-toulouse.fr)

# Enhanced Dielectric Relaxation in Self-Organized Layers of Polypeptides Coupled to Platinum Nanoparticles: Temperature Dependence and Effect of Bias Voltage

Louis Merle, Ghada Manai, Adeline Pham, Sébastien Lecommandoux, Philippe Demont, Colin Bonduelle, Simon Tricard, Adnen Mlayah, and Jérémie Grisolia\*

**ABSTRACT:** Using alternative current impedance spectroscopy, we investigate the dynamical conductivity of hybrid nanomaterials composed of helical polypeptide layers containing platinum nanoparticles (PtNP). The electrical characteristics of the self organized poly( $\gamma$  benzyl L glutamate) (PBLG) in bidimensional lamellar assembly in the presence of Pt nanoparticles are well modeled and described by a single equivalent circuit of parallel resistance and capacitance. The latter are determined using a comparison between the measured and calculated Nyquist plots, which allows extracting the characteristic relaxation time and frequency of the dipolar relaxation process. We found that the relaxation frequency in the PBLG–PtNP hybrid materials is enhanced by 4 orders of magnitudes compared to pure PBLG, which indicates a much faster dielectric relaxation in PBLG–PtNP due to dipole orientation and dipole–dipole interactions. The temperature dependence of the relaxation time is analyzed using Arrhenius plots, from which the activation energy of the relaxation process is found to be around 0.1 eV. Such a value close to the peptide vibration energy of the PBLG indicates a vibration assisted relaxation process and a polaronic charge transport mechanism. An advantage of the PBLG–PtNP nanocomposite material is that the activation energy can be finely tuned by the PBLG degree of polymerization. Finally, an important outcome of this work is the investigation of the dielectric relaxation process in PBLG–PtNP under applied DC bias. We found that the activation energy decreases with increasing bias voltage for all degrees of polymerization of the PBLG molecule. This effect is interpreted in terms of electric field induced alignment of the dipoles and of increased mobility of the polaronic charge carriers. The presence of piezoelectricity in the hybrid material gives the possibility to use the DC bias as a simple mean of monitoring the dynamical conductivity involving polaronic states.



## INTRODUCTION

Nanocomposites are defined here as hybrid materials where both organic and inorganic phases coexist and exhibit a spatial organization at the nanoscale. These two phases present complementary properties (magnetic, electronic, photonic)<sup>1</sup> generated by a synergy between the different species. These novel materials are very promising for applications in strain sensors,<sup>2</sup> or memories,<sup>3</sup> and more generally in nano electronics.<sup>4,5</sup> In addition to the nature of the components of the hybrid material, the structural organization—at the nanoscale—brings out new mechanical<sup>6</sup> and electrical properties.<sup>7</sup> A recent strategy to provide nanocomposites is to co assemble peptidic polymers and metallic nanoparticles (NPs).<sup>8</sup> Indeed, polypeptide polymers present an ordered secondary structure in  $\alpha$  helix, in  $\beta$  sheet, or a disordered structure in random coil,<sup>9</sup> each conformation having its intrinsic properties (hydrodynamic volume, rigidity, solubility, van der Waals bonding),<sup>9–11</sup> and is responsible for structural organization up to the macroscopic scale.<sup>12</sup> A particularity of  $\alpha$  helical

polypeptides is the existence of a piezoelectric character<sup>13</sup> if the electric dipoles are parallel to the helix axis. In the case of Pt nanoparticles (NP) and poly( $\gamma$  benzyl L glutamate) (PBLG) in  $\alpha$  helix, the system presents a lamellar organization of the PBLG molecules.<sup>8</sup> In such a system, the  $\alpha$  helices aligned with each other to form lamellae separated by lines of nanoparticles, the surface of which interacts with functional groups of the PBLG by coordination interactions. The multiscale characteristics of these nanocomposites, composed of conductive and insulating domains, strongly impact their dielectric properties such as dipolar relaxation and dynamical

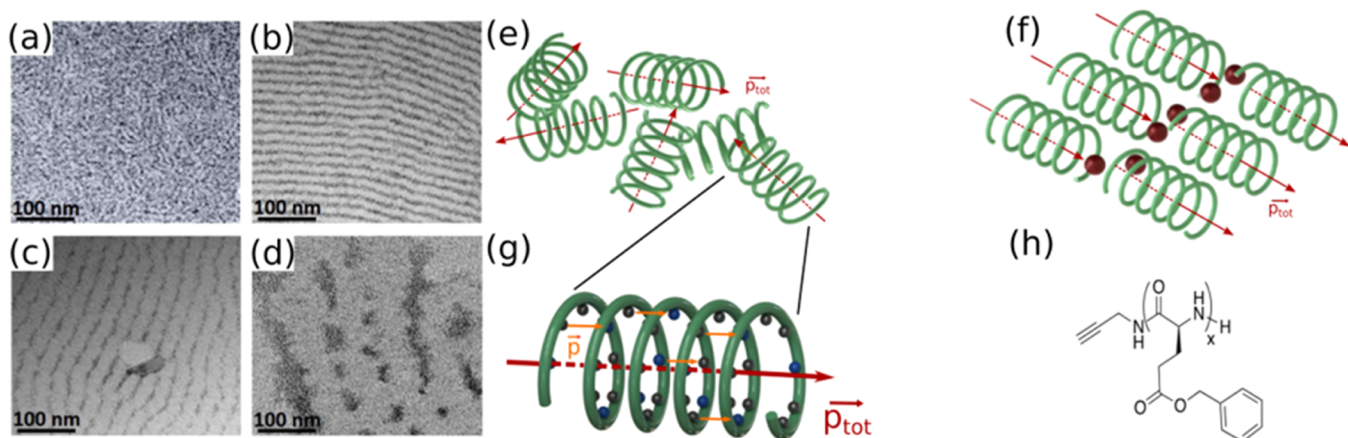


**Figure 1.** (a–d) TEM images of PBLG–PtNP for different polymerization degrees (DP): (a) PBLG1 (DP 69), (b) PBLG2 (DP 120), (c) PBLG3 (DP 217), (d) PBLG4 (DP 481). Regions of high density of Pt NPs appear as dark regions containing NPs, whereas the regions of pure PBLG appear bright. Schematic of the helical structure of PBLG without Pt NP (e) and in the presence of Pt (f). PBLG is represented in green, and the Pt NP in red spheres. (g) Schematic representation of an  $\alpha$  helix PBLG molecule, orange arrows describe the resulting electrical dipole moments carried by the peptide bond. The red arrows represent the total electrical dipole moment carried by the chain. (h) Chemical representation of PBLG, with  $x$  the polymerization degree (DP).

conductivity, which can be finely probed using AC impedance spectroscopy. It is therefore interesting to investigate the dynamical transport mechanisms in these systems for the fundamental understanding of the correlation between electrical transport and piezoelectric properties and the structural organization of the hybrid Pt/PBLG material.

In this work, we focus on the dielectric response of different hybrid materials composed of PBLG in  $\alpha$  helix conformation and Pt NP using AC impedance spectroscopy.<sup>14</sup> Impedance spectroscopy allows the understanding of the transport and relaxation mechanisms that take place in the material, through the activation energy of the process. The activation energy of the relaxation process responsible for the dynamical conductivity depends on the materials and on the nature of the conduction processes. It can range from tens of meV in the case of Pd–ZrO<sub>2</sub><sup>15,16</sup> to several hundreds of meV in hybrid polymer systems, such as poly(vinyl alcohol) containing barium zirconium titanate ceramic.<sup>17</sup> The measured impedance spectra are interpreted using equivalent electrical circuits combining the PBLG–PtNP resistance and capacitance as well as the contact electrode resistance. The studied system PBLG–PtNP can then be considered as a granular system composed of insulating and conducting phases. The temperature dependence of the so extracted relaxation time allows determining the activation energy. In the present work, we focus on the activation energy of the relaxation process responsible for the dynamical conductivity of the PBLG–PtNP layers. In particular, we investigate the change of the activation energy with the degree of polymerization (DP) of the PBLG molecules and its relation on an applied DC bias voltage.

## METHODS

Platinum nanoparticles of diameter  $1.2 \pm 0.3$  nm were synthesized by decomposition of Pt<sub>2</sub>(dba) in tetrahydrofuran (THF) under an atmosphere of CO, followed by complete elimination of the organic dibenzylideneacetone (dba) residue by washing with pentane.<sup>18</sup> Poly( $\gamma$  benzyl L glutamate) (PBLG) was obtained by ring opening polymerization of  $\gamma$  benzyl L glutamate N carboxyanhydride monomers using propargylamine as an initiator in dimethylformamide.<sup>19</sup> The

polymerization degree (DP) of the PBLG was controlled during the synthesis by adjusting the stoichiometry of the initiator (I) compared to the monomer (M; M/I ratio or theoretical DP). With theoretical DP values of 60, 120, 240, and 480, the labeled samples PBLG1, PBLG2, PBLG3, and PBLG4 have, respectively, DP values of 69, 120, 217, and 481. The hybrid PBLG–PtNP composite is obtained by mixing the Pt nanoparticles with PBLG in THF. Solutions of PtNPs and of PBLG were mixed and stirred for 2 h at an equivalent number of 0.5 (equivalent number is the ratio between the monomer unit and the Pt atom quantities), as the assembly process occurs at an optimum relative ratio of polymer *vs* nanoparticle equals 0.5 equiv.<sup>8</sup> The PBLG–PtNP composite formed bidimensional layers already present in solution.<sup>8</sup>

Pure PBLG and PBLG–PtNP were tested using a T shaped architecture with two copper pads connected to interdigitated  $250 \times 100 \times 0.1 \mu\text{m}^3$  comb electrodes separated by  $5 \mu\text{m}$ .<sup>20</sup> Electric characteristics were measured using a Janis ST 500 1 cryogenic probe station. The sample temperature was monitored in the 290–350 K range using a Lakeshore 350 controller operating at a 2 K/min heating rate. Impedance spectroscopy measurements were performed using a Keysight Impedance Analyzer EA4990A in the 20 Hz to 5 MHz frequency range with a 500 mV AC voltage and under applied bias voltage ranging from 0 to 2.5 V.

## RESULTS AND DISCUSSION

**Degree of Polymerization (DP).** Figure 1a–d displays transmission electron microscopy (TEM) images of the hybrid PBLG–PtNP material obtained with the different polymerization degrees of PBLG. The regions of high and low densities of Pt NPs in PBLG are visible in Figure 1a–d as alternated dark and bright areas, respectively. As shown in a previous study,<sup>8</sup> the size of PBLG areas, with low density of Pt NPs, increases with increasing DP as  $d = 0.095 \times \text{DP}$ .

One can notice that the organization of the PBLG–PtNP composite film evolves with DP from a short range (sub 10 nm) ordered structure (PBLG1) to a periodic alternation of dark and bright regions of Pt NP rich and Pt NP free region of PBLG, particularly for PBLG2 and PBLG3. Indeed, a

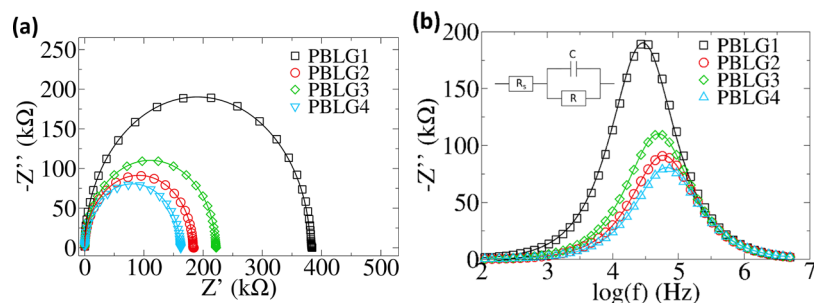


**Figure 2.** Experimental (symbols) Nyquist impedance plots (*i.e.*,  $Z'$  vs  $-Z''$  in  $k\Omega$ ) of PBLG–PtNP and fit (straight lines) for PBLG1, PBLG2, PBLG3, and PBLG4. (b)  $-Z''$  as a function of frequency with experimental data (symbols) and Lorentzian fit (straight lines). The electrical equivalent circuit used for the modeling of the frequency dependent impedance is shown in the inset.

characteristic feature of PBLG–PtNP is its lamellar structural organization at a mesoscopic scale<sup>8</sup> (Figure 1b–d,f), which arises from areas of well aligned PLBG chains, with an  $\alpha$  helix structure<sup>21</sup> (Figure 1g) bridged by areas containing Pt NPs and PBLG in random coil. On the contrary, the pure PBLG film exhibits no organization (Figure 1e). The presence of Pt NPs leads to the lamellar structure of the PBLG–PtNP composite with optimum DP of 120 and 217 (respectively, PBLG2 and PBLG3) (Figures 1b,c and SI 1). For PBLG4, the Pt NPs agglomerate in rather large (sub 100 nm) and isolated packets that results in a less ordered, but still aligned, structure (Figure 1d).

Monomer units of the PBLG carry a resulting electrical dipole on the peptide bonds of the  $\alpha$  helix. The repetition of monomer units, in helical conformation, results in a large electrical dipole and hence the PBLG acquires piezoelectric properties.<sup>15</sup> However, the dipole orientation is random in the disordered phase (PBLG without Pt NPs, Figure 1e) and the average macrodipole cancels out. However, in the ordered phase (Figure 1f), due to the lamellar structure of the composite PBLG–PtNP film, the dipoles attached to each  $\alpha$  helix PBLG chain are aligned and sum up, thus giving rise to a macrodipole at a macroscopic scale. Piezoelectricity may thus emerge as a result of the lamellar self organization of the composite PBLG–PtNP material. Moreover, the PBLG–PtNP composite material is a granular system with insulating (PBLG) and conducting (PtNP) components, the electrical transport properties of which can be fully characterized using impedance spectroscopy.<sup>15</sup>

Figure 2 shows room temperature impedance spectra acquired in the 20 Hz to 5 MHz frequency range with 500 mV AC voltage and 0 V DC bias. Figure 2a presents the Nyquist impedance plots of PBLG–PtNP for the investigated DP values. Each sample exhibits a semicircle whose radius gives the impedance modulus, which is in the order of hundreds of  $k\Omega$ . A remarkable point is that regardless of the DP, the impedance of the PBLG–PtNP layers is 4 orders of magnitude smaller than the one measured on a pure PBLG layer (*i.e.*, without Pt NPs), which is around several  $G\Omega$  (Figure SI 2, Supporting information). These measurements clearly indicate the self assembly created by the synergy of PBLG, and Pt NPs strongly enhance the dynamical conductivity of the composite material reducing its electrical impedance by 4 orders of magnitude. PBLG1 exhibits the lowest degree of organization (Figure 1) and has the largest impedance (around 400  $k\Omega$  at low frequency), as shown in Figure 2a. The impedance of the more ordered layers (PBLG2–4) is reduced by roughly a factor of 2 compared to

PBLG1 (Figure 2a). However, the impedance measured for PBLG3 (225  $k\Omega$ ) is larger than the one measured for PBLG2 (175  $k\Omega$ ). This inversion of conductivity is attributed to structural defects in the organization of the layer. Indeed, the disorder in the lamellar organization, *i.e.*, variations in orientations of the lamellae separated by grain boundaries and defects in their contact to the electrodes, may reduce the conductivity of the layer and explain the nonmonotonic evolution of the Nyquist plots with the degree of polymerization (Figure 2a).

Figure 2b shows the spectra of the imaginary part  $Z''$  of the impedance as a function of frequency measured for the PBLG–PtNP layers. First, each spectrum consists of a single Lorentzian like resonance peak, as confirmed by the plot of the electrical modulus vs  $\log(f)$  (see Figure SI 3), indicating a single electrical relaxation phenomenon responsible for the dynamical conductivity response of the composite layers. It is characterized by well defined resonance frequency  $f_c$  and relaxation time  $\tau$ . An  $f_c$  value of 30 kHz corresponding to  $\tau = 33 \mu s$  is found for PBLG1. For all other samples, from PBLG2 to 4, the resonance frequency increases with respect to PBLG1 and reaches  $f_c = 65$  kHz ( $\tau = 15 \mu s$ ) for PBLG4. One can notice that PBLG3 exhibits an  $f_c$  of 60 kHz, which is slightly higher than that observed for PBLG2,  $f_c = 50$  kHz, which confirms that not only the DP but also the ordering of the layer may impact the relaxation dynamics, as already noticed in Nyquist plots (Figure 2a).

It is worth mentioning that the resonance frequencies observed here for the PBLG–PtNP composite layers are much larger (at least 4 orders of magnitudes) than the one estimated for pure PBLG (Figure SI 2, Supporting Information). This difference indicates that the ordering of the PBLG molecules in the PBLG–PtNP composite material strongly impacts not only the magnitude (Figure 2a) of the electrical impedance but also the relaxation dynamics (Figure 2b) of the dipoles carried by each PBLG molecule (Figure 1g). Indeed, we suggest that the ordering of the PBLG molecules in the lamellar structure (Figure 1f) leads to dipoles alignment and to efficient dipole–dipole interaction, and hence to a blockade of the reorientation of the dipoles. As a consequence, the relaxation process of the interacting dipoles occurs at a much higher frequency, compared to the case of randomly oriented PBLG molecules (*i.e.*, pure PBLG), thus reflecting the structural ordering of the PBLG molecules in the PBLG–PtNP composite material.

The semicircular shape of Nyquist plots (Figure 2a) indicates that the electrical conductivity of the PBLG–PtNP layers can be modeled using an electrical equivalent circuit consisting of a parallel resistance  $R$  and capacitance  $C$ .<sup>15</sup> An

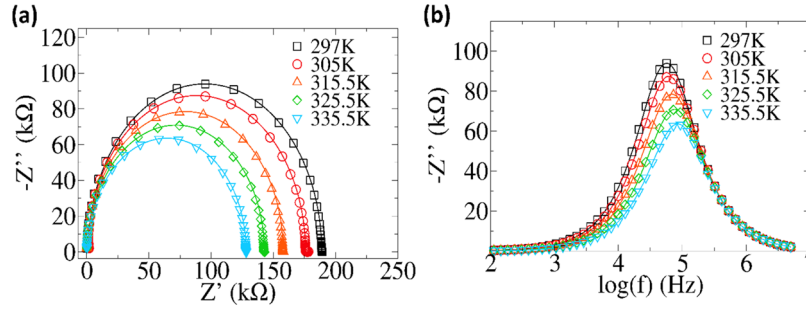


**Figure 3.** (a) Experimental (symbols) Nyquist impedance plots ( $Z$  in  $k\Omega$ ) of PBLG2 and fit (straight lines) for temperatures between 297 and 335.5 K. (b)  $-Z''$  as a function of frequency with experimental data (symbols) and fit (straight lines) for various temperatures.

additional series resistance  $R_s$  is included to account for the electrode's resistance. The complex impedance of the equivalent electrical circuit is then defined as

$$Z(\omega) = Z'(\omega) + jZ''(\omega) = R_s + \frac{R}{1 + jRC\omega} \quad (1)$$

where  $Z'$  and  $Z''$  are, respectively, the real and imaginary parts of the impedance at angular frequency  $\omega$ ,  $R$ ,  $C$ , and  $R_s$ . These latter values are determined using a least squares fit of the calculated impedance (eq 1) to the measured one. The relaxation time is hence obtained as  $\tau = RC = \frac{1}{2\pi f_c}$ .

**Temperature Effect.** Figure 3a displays temperature dependent Nyquist plots for the PBLG2 composite with no applied DC bias and shows that the radius of the semicircles and the total impedance of the sample decrease with increasing temperature. The samples PBLG1, PBLG3, and PBLG4 exhibit a similar behavior.

This is corroborated by the temperature dependence of the resistance  $R$  and capacitance  $C$  (see Figure SI 4). These latter values were extracted from Nyquist plots using a fitting procedure based on eq 1. We found that the resistance decreases by 0.8%/K, whereas the capacitance decreases by only  $4 \times 10^{-3}\%$ /K with increasing temperature. This observation indicates that the temperature dependence of the impedance is mainly due to its resistive component and that the relaxation process is thermally activated. Correlatively, the impedance resonance peak shifts toward higher frequencies with increasing temperature (Figure 3b), which reveals that the relaxation process at work is getting faster, thus confirming its thermally activated nature. Indeed, because of its lamellar structure, PBLG–PtNP presents a dielectric component, the resistance of which may decrease with increasing temperature due to thermally enhanced carrier mobility.<sup>22</sup> Such an enhancement can occur in several charge transport mechanisms involving hopping between trapping sites, quantum tunneling, and formation of large polarons.<sup>23–25</sup>

The change of the resonance peak frequency  $f_c$  as a function of temperature extracted from the spectra in Figure 3b allows the determination of the activation energy of the relaxation phenomenon, responsible for the dynamical conductivity of our composite PBLG–PtNP nanomaterials. Assuming that  $f_c$  follows an Arrhenius law,<sup>17</sup> its temperature dependence is given by

$$f_c = f_0 e^{-E_a/kT} \quad (2)$$

where  $f_0$  is the resonance frequency at a high temperature,  $k$  is the Boltzmann constant, and  $E_a$  is the activation energy. As

shown by the Arrhenius plots (Figure 4), the temperature dependence  $f_c$  is well described using a single activation energy, which confirms that a single conduction mechanism can account for the experimental data.

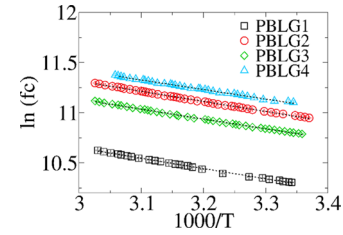


**Figure 4.**  $\ln(f_c)$  as a function of  $1000/T$  for PBLG1, PBLG2, PBLG3, and PBLG4 at a 0 DC bias voltage. Symbols represent experimental data, and lines are linear fits.

This single conduction mechanism is in contrast to the one pointed out in composite materials involving polydispersed nanoparticles<sup>26</sup> or particles of several micrometers in size,<sup>27</sup> where two activation energies are generally found; one is associated with the grains themselves and the other one with the grain boundary. In our samples, the nanometer size of the Pt NPs (1.2 nm) leads to a grain capacitance of a few fF only<sup>20</sup> and therefore to relaxation frequencies of NPs above 5 MHz. Grain effects are thus negligible here. Only the activation energy of the dielectric relaxation process involving the PBLG is thus measurable in our frequency range. The activation energies extracted for the PBLG–PtNP samples with PBLG1–4 are, respectively, 0.102, 0.105, 0.098, and 0.095 eV ( $\pm 0.001$  eV). These values lie in the 900–1000  $\text{cm}^{-1}$  range, *i.e.*, close to the vibration frequency of the stretching mode of the CN bond (*ca.* 1200  $\text{cm}^{-1}$ , *i.e.*, 0.15 eV).<sup>8</sup> The fact that the obtained activation energies are close to that of the peptide group vibrations strongly suggests a thermally activated dipole relaxation process. The relaxation rate is therefore expected to be proportional to the thermal population of vibration modes of the peptide group, which is given by the Bose–Einstein factor. The latter can be approximated by  $\exp\left(\frac{-h\omega}{kT}\right)$  in the considered temperature range. Comparison with Arrhenius law (eq 2) strongly suggests that the relaxation frequency is indeed proportional to the thermal population of the peptide vibrations and that the relaxation process and the dynamical conductivity are assisted by such vibrations in our PBLG–PtNP nanomaterials.

**DC Bias Voltage Effect.** The piezoelectric properties of the synthesized PBLG–PtNP nanomaterials were investigated by impedance spectroscopy measurements under various

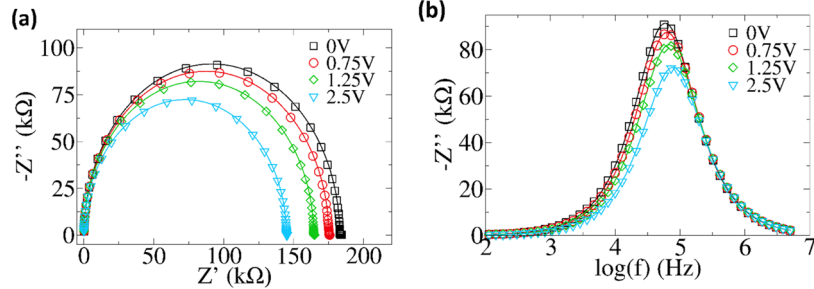


**Figure 5.** (a) Room temperature experimental (symbols) Nyquist impedance plots ( $Z$  in  $k\Omega$ ) of PBLG–PtNP with PBLG2 and fitted (eq 1) plots (lines) for DC bias voltage ranging from 0 to 2.5 V under 300 K. (b) Room temperature measured spectra of  $-Z''$  as a function of frequency with spectra experimental data (symbols) and the corresponding fits (straight lines) for DC bias voltage ranging from 0 to 2.5 V.

applied DC bias voltages. Figure 5 shows typical experimental results (here displayed only for the PBLG2). Both Nyquist plots (Figure 5a) and  $-Z''$  impedance spectra (Figure 5b) are displayed.

The impedance decreases with increasing DC bias voltage (Figure 5a) following a linear variation with a characteristic slope of  $-10 k\Omega/V$ . Moreover, the resonance frequency of the impedance peak (Figure 5b) increases linearly by  $7.6 kHz/V$  with increasing bias voltage. All investigated hybrid PBLG–PtNP nanomaterials exhibit a similar behavior with respect to the applied bias voltage. It is worthwhile to mention that the sensitivity of PBLG–PtNP to an applied external electric field is not observed in the pure PBLG reference sample (Figure SI 5), *i.e.*, without Pt nanoparticles. The dependence on the DC bias is explained by the lamellar structure of PBLG–PtNP (Figure 1f), which favors the alignment of the microscopic dipoles and thus the emergence of a macroscopic polarization (Figure 1) that can be modulated by an applied external field. No such macroscopic polarization is present in the pure PBLG sample. To go deeper into the understanding of the effect of the applied field on the transport properties and relaxation dynamics, we have performed temperature dependent impedance spectroscopy measurements under applied DC bias voltage (Figure 6).

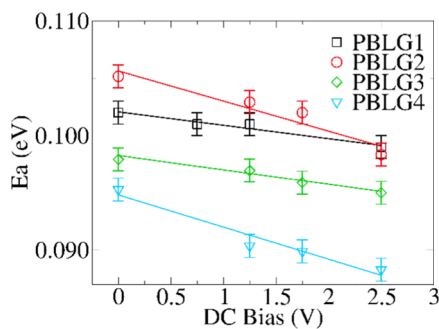


**Figure 6.** Activation energy ( $\pm 0.001$  eV) vs DC bias voltage (V) extracted from Arrhenius law. To each type of symbol is associated extracted activation energies of PBLG1–4 and corresponding fit (straight lines).

In this way, we are able to extract the dependence of the activation energy (eq 2, Figure SI 6) on the applied bias voltage. The so obtained results are presented in Table 1.

At zero DC bias, the measured activation energy is of the order of 0.1 eV for all DPs and decreases almost linearly with increasing bias voltage with characteristic slopes between  $-0.012$  eV/V (for PBLG1) and  $-0.028$  eV/V (for PBLG4).

**Table 1. Activation Energy of PBLG1–4 and the Derivative of the Activation Energy with DC Bias Voltage**

DC bias (V)	activation energy (eV)			
	PBLG1	PBLG2	PBLG3	PBLG4
0	0.102	0.105	0.098	0.095
0.75	0.101			
1.25	0.101	0.103	0.097	0.090
1.75		0.102	0.096	0.089
2.5	0.099	0.098	0.095	0.088
$dE_a/dU$ (eV/V)				
PBLG1	PBLG2	PBLG3	PBLG4	
0.012	0.026	0.013	0.028	

The drop of the activation energy with applied DC bias is interpreted in terms of orientation of the dipoles, carried by the PBLG molecules, along the direction of the imposed DC electric field. The electric field induced alignment of the dipoles may in turn decrease the energy barrier of the localized polarons, thus leading to an increased carrier mobility and a lowering of the impedance as observed in Figure 5a. One can notice that, for PBLG3 and PBLG4, the activation energy decreases by only 0.001 eV, for DC bias increasing from 1.75 to 2.5 V, which suggests a possible saturation of the effect corresponding to a full alignment of the dipoles with the applied DC electric field. Such an effect could be related to the spatial distribution of the PBLG molecules in the lamellar structure with several orientation domains separated by grain boundaries.

## CONCLUSIONS

In summary, we have investigated the dynamical conductivity of a polypeptide–nanoparticle nanocomposite using impedance spectroscopy measurements. The lamellar organization of PBLG with Pt NPs provides electrical dipole moments at the scale of the polymer chains. The increase of the PBLG relaxation frequency by 4 orders of magnitudes in the presence of Pt NP underlines the importance of the supramolecular organization. Such an organization facilitates the orientation and alignment of the dipoles, with activation energies of the order of 0.1 eV, comparable to the ones reported for hybrid granular materials. Besides, the high polymerization degree of the PBLG molecules favors the lamellar organization and the emergence of coherent polarization domains. Indeed, the higher the molar mass of the polymer, the higher the dipole moment of the chains and the lower the nanocomposite activation energy. The application of a DC bias voltage also decreases the activation energy, by orienting the electric

dipoles along the applied field. Self assembly of hybrid materials is a fundamental approach to synthesize nano composites, with physical responses comparable to the ones of inorganic compounds, but with the flexibility afforded by the polymer and nanoparticle chemistries. The presented work unravels the impact of the organization of the PBLG–PtNP hybrid material on its electrical parameters, which is useful for the development of novel devices in nanoelectronics.

## ■ ASSOCIATED CONTENT

### ● Supporting Information

The Supporting Information is available free of charge at <https://pubs.acs.org/doi/10.1021/acs.jpcc.1c06457>.

TEM images of PBLG–PtNP, Nyquist plot of unstructured PBLG2, imaginary part of the electrical modulus  $M$  as a function of frequency in a semilog scale, capacitance and resistance measured as a function of temperature, Nyquist plot of unstructured PBLG2 for DC bias voltage between 0 and 2.5 V, and Arrhenius plots of the resonance peak frequency  $f_c$  for DC bias voltage between 0 and 2.5 V and for PBLG1, PBLG2, PBLG3, and PBLG4 (PDF)

## ■ AUTHOR INFORMATION

### Corresponding Author

J r mie Grisolia – LPCNO, Universit  de Toulouse, INSA, CNRS, UPS, 31077 Toulouse, France;  
Email: [jeremie.grisolia@insa-toulouse.fr](mailto:jeremie.grisolia@insa-toulouse.fr)

### Authors

Louis Merle – LPCNO, Universit  de Toulouse, INSA, CNRS, UPS, 31077 Toulouse, France

Ghada Manai – LPCNO, Universit  de Toulouse, INSA, CNRS, UPS, 31077 Toulouse, France

Adeline Pham – LPCNO, Universit  de Toulouse, INSA, CNRS, UPS, 31077 Toulouse, France

S bastien Lecommandoux – LCPO, Universit  de Bordeaux, CNRS, Bordeaux INP, LCPO UMR 5629, F 33600 Pessac, France

Philippe Demont – CIRIMAT, Universit  Toulouse–Paul Sabatier, 31062 Toulouse, France

Colin Bonduelle – LCPO, Universit  de Bordeaux, CNRS, Bordeaux INP, LCPO UMR 5629, F 33600 Pessac, France;  
[orcid.org/0000-0002-7213-7861](https://orcid.org/0000-0002-7213-7861)

Simon Tricard – LPCNO, Universit  de Toulouse, INSA, CNRS, UPS, 31077 Toulouse, France; [orcid.org/0000-0002-0061-8578](https://orcid.org/0000-0002-0061-8578)

Adnen Mlayah – CEMES, Universit  de Toulouse, CEMES CNRS, 31055 Toulouse, France; LAAS, Universit  de Toulouse, CNRS, UPS, 31400 Toulouse, France;  
[orcid.org/0000-0003-1129-8220](https://orcid.org/0000-0003-1129-8220)

Complete contact information is available at: <https://pubs.acs.org/doi/10.1021/acs.jpcc.1c06457>

### Notes

The authors declare no competing financial interest.

## ■ ACKNOWLEDGMENTS

The authors thank S. Raffy and C. Midelet for fruitful discussions on the support of fitting and graphing. Financial support from Universit  de Toulouse (NaSAPeP grant APR), from CNRS (MITI interdisciplinary programs, COCOPIE

project) and from Agence Nationale de la Recherche (MOSC grant ANR 18 CE09 0007) is acknowledged. This study has been partially supported through the EUR grant NanoX no. ANR 17 EURE 0009 in the framework of the Programme des Investissements d’Avenir.

## ■ REFERENCES

- (1) Kao, J.; Thorkelsson, K.; Bai, P.; Rancatore, B. J.; Xu, T. Toward functional nanocomposites: taking the best of nanoparticles, polymers, and small molecules. *Chem. Soc. Rev.* 2013, 42, 2654–2678.
- (2) Kim, Y. J.; Cha, J. Y.; Ham, H.; Huh, H.; So, D. S.; Kang, I. Preparation of piezoresistive nano smart hybrid material based on graphene. *Curr. Appl. Phys.* 2011, 11, S350–S352.
- (3) Verbakel, F.; Meskers, S. C. J.; Janssen, R. A. J. Electronic memory effects in diodes from a zinc oxide nanoparticle polystyrene hybrid material. *Appl. Phys. Lett.* 2006, 89, No. 102103.
- (4) Huynh, W. U. Hybrid Nanorod Polymer Solar Cells. *Science* 2002, 295, 2425–2427.
- (5) Balazs, A. C.; Emrick, T.; Russell, T. P. Nanoparticle Polymer Composites: Where Two Small Worlds Meet. *Science* 2006, 314, 1107–1110.
- (6) Crosby, A. J.; Lee, J. Polymer Nanocomposites: The “Nano” Effect on Mechanical Properties. *Polym. Rev.* 2007, 47, 217–229.
- (7) Yi, C.; Yang, Y.; Liu, B.; He, J.; Nie, Z. Polymer guided assembly of inorganic nanoparticles. *Chem. Soc. Rev.* 2020, 49, 465–508.
- (8) Manai, G.; et al. Bidimensional lamellar assembly by coordination of peptidic homopolymers to platinum nanoparticles. *Nat. Commun.* 2020, 11, No. 2051.
- (9) Bonduelle, C. Secondary structures of synthetic polypeptide polymers. *Polym. Chem.* 2018, 9, 1517–1529.
- (10) Sharp, M. Dielectric Study of Dilute Solutions of Poly  $\gamma$  benzyl L glutamate. *J. Chem. Soc. A* 1970, 1596–1601.
- (11) Kratzm ller, T.; Appelhans, D.; Braun, H. G. Ultrathin Microstructured Polypeptide Layers by Surface initiated Polymerization on Microprinted Surfaces. *Adv. Mater.* 1999, 11, 555–558.
- (12) Cai, C.; Lin, J.; Lu, Y.; Zhang, Q.; Wang, L. Polypeptide self assemblies: nanostructures and bioapplications. *Chem. Soc. Rev.* 2016, 45, 5985–6012.
- (13) Jaworek, T.; Neher, D.; Wegner, G.; Wieringa, R. H.; Schouten, A. J. Electromechanical Properties of an Ultrathin Layer of Directionally Aligned Helical Polypeptides. *Science* 1998, 279, 57–62.
- (14) Kuwabara, T.; Kawahara, Y.; Yamaguchi, T.; Takahashi, K. Characterization of Inverted Type Organic Solar Cells with a ZnO Layer as the Electron Collection Electrode by ac Impedance Spectroscopy. *ACS Appl. Mater. Interfaces* 2009, 1, 2107–2110.
- (15) Bakkali, H.; Dominguez, M.; Battle, X.; Labarta, A. Universality of the electrical transport in granular metals. *Sci. Rep.* 2016, 6, No. 29676.
- (16) Bakkali, H.; Dominguez, M.; Battle, X.; Labarta. Equivalent circuit modeling of the ac response of Pd ZrO<sub>2</sub> granular metal thin films using impedance spectroscopy. *J. Phys. D: Appl. Phys.* 2015, 48, No. 335306.
- (17) Senthil, V.; Badapanda, T.; Kumar, S. N.; Kumar, P.; Panigrahi, S. Relaxation and conduction mechanism of PVA: BYZT polymer composites by impedance spectroscopy. *J. Polym. Res.* 2012, 19, No. 9838.
- (18) Tricard, S.; et al. Chemical tuning of Coulomb blockade at room temperature in ultra small platinum nanoparticle self assemblies. *Mater. Horiz.* 2017, 4, 487–492.
- (19) Schatz, C.; Louguet, S.; Meins, J. F. L.; Lecommandoux, S. Polysaccharide block polypeptide Copolymer Vesicles: Towards Synthetic Viral Capsids. *Angew. Chem., Int. Ed.* 2009, 48, 2572–2575.
- (20) Nesser, H.; Grisolia, J.; Alnasser, T.; Viallet, B.; Ressler, L. Towards wireless highly sensitive capacitive strain sensors based on gold colloidal nanoparticles. *Nanoscale* 2018, 10, 10479–10487.
- (21) Chang, Y. C.; Frank, C. W.; Forstmann, G. G.; Johannsmann, D. Quadrupolar and polar anisotropy in end grafted  $\alpha$  helical poly( $\gamma$



benzyl L glutamate) on solid substrates. *J. Chem. Phys.* **1999**, *111*, 6136–6143.

(22) Saha, T. K.; Purkait, P. Investigations of Temperature Effects on the Dielectric Response Measurements of Transformer Oil Paper Insulation System. *IEEE Trans. Power Delivery* **2008**, *23*, 252–260.

(23) Coşkun, M.; Polat, O.; Coşkun, F. M.; Durmuş, C.; Çağlar, M.; Türüt, A. Frequency and temperature dependent electrical and dielectric properties of LaCrO<sub>3</sub> and Ir doped LaCrO<sub>3</sub> perovskite compounds. *J. Alloys Compd.* **2018**, *740*, 1012–1023.

(24) Nasri, S.; Megdiche, M.; Gargouri, M. DC conductivity and study of AC electrical conduction mechanisms by non overlapping small polaron tunneling model in LiFeP<sub>2</sub>O<sub>7</sub> ceramic. *Ceram. Int.* **2016**, *42*, 943–951.

(25) Morita, T.; Kimura, S. Long Range Electron Transfer over 4 nm Governed by an Inelastic Hopping Mechanism in Self Assembled Monolayers of Helical Peptides. *J. Am. Chem. Soc.* **2003**, *125*, 8732–8733.

(26) Bakkali, H.; Dominguez, M. Differential conductance of Pd ZrO<sub>2</sub> thin granular films prepared by RF magnetron sputtering. *EPL* **2013**, *104*, No. 17007.

(27) Coşkun, M.; Polat, O.; Coşkun, F. M.; Durmuş, C.; Çağlar, M.; Türüt, A. The electrical modulus and other dielectric properties by the impedance spectroscopy of LaCrO<sub>3</sub> and LaCr<sub>0.90</sub>Ir<sub>0.10</sub>O<sub>3</sub> perovskites. *RSC Adv.* **2018**, *8*, 4634–4648.